Biomed Microdevices (2011) 13:221–230
DOI 10.1007/s10544-010-9487-1

Electrochemically switchable platform for the micro-patterning and release of heterotypic cell sheets

Orane Guillaume-Gentil · Michael Gabi · Marcy Zenobi-Wong · Janos Vörös

Published online: 6 November 2010

Abstract This article describes a dynamic platform in which the biointerfacial properties of micro-patterned domains can be switched electrochemically through the spatio-temporally controlled dissolution and adsorption of polyelectrolyte coatings. Insulating SU-8 micro-patterns created on a transparent indium tin oxide electrode by photolithography allowed for the local control over the electrochemical dissolution of polyelectrolyte mono- and multilayers, with polyelectrolytes shielded from the electrochemical treatment by the underlying photoresist stencil. The platform allowed for the creation of micro-patterned cell co-cultures through the electrochemical removal of a non-fouling polyelectrolyte coating and the localized adsorption of a cell adhesive one after attachment of the first cell population. In addition, the use of weak adhesive polyelectrolyte coatings on the photoresist domains allowed for the detachment of a contiguous heterotypic cell sheet upon electrochemical trigger. Cells grown on the ITO domains peeled off upon electrochemical dissolution of the sacrificial polyelectrolyte substrate, whereas adjacent cell areas on the insulated weakly adhesive substrate easily detached through the contractile force generated by neighboring cells. This electrochemical strategy for the micro-patterning and detachment of heterotypic cell sheets combines simplicity, precision and versatility, and presents great prospects for the creation of cellular constructs which mimic the cellular complexity of native tissues.

O. Guillaume-Gentil · M. Gabi · M. Zenobi-Wong · J. Vörös (✉)
Laboratory of Biosensors & Bioelectronics,
Institute for Biomedical Engineering, ETH Zurich,
Gloriastrasse 35,
8092 Zurich, Switzerland
e-mail: janos.voros@biomed.ee.ethz.ch

Keywords Indium tin oxide electrode · SU-8 photoresist · Micro-patterning · Photolithography · Cell co-cultures · Heterotypic cell sheet engineering

1 Introduction

Polyelectrolyte-modified surfaces offer a high versatility for the design of optimal biointerfaces for a variety of biomedical applications. Polyelectrolytes in aqueous solutions adsorb spontaneously onto oppositely charged surfaces, hence facile coating processes applicable to any surface geometry (e.g. dip-and-rinse, spraying), and polyelectrolyte multilayers can be easily assembled through the alternate deposition of polycations and polyanions, allowing for the formation of structures ranging from nano-droplets to micrometer thick continuous films (Decher 1997; Picart et al. 2001, 2002; Schlenoff et al. 2000). The intrinsic properties of the polyelectrolytes, the physico-chemical properties of the cover medium, as well as the deposition parameters can dramatically affect the multilayer's internal structure, allowing for a tight tuning of the physical, chemical and mechanical properties of the coating. This technique can be used to tune the adhesive properties of a surface, from totally non-fouling to highly cell adhesive (through specific or unspecific interactions) (Tang et al. 2006; Boudou et al. 2010; VandeVondele et al. 2003; Elbert and Hubbell 1998). In addition to the multilayer's composition and the use of appropriate build-up conditions, the biological properties of polyelectrolyte coatings can also be modulated with bioactive moieties, embedded in the coating or adsorbed on the top of it (Boudou et al. 2010). The surface modification with polyelectrolytes therefore represents a simple approach of great potential for the design of desired interfacial properties.

Recently, polyelectrolyte-modified surfaces were successfully applied as new platforms for cell sheet engineering, i.e. for the growth and subsequent non-invasive harvesting of entire cell monolayers (Guillaume-Gentil et al. 2008). Coatings made of poly-L-lysine (PLL) and hyaluronic acid (HA) presented weak cell adhesive properties (Weder et al. 2010), allowing for spontaneous, mechanical cell sheet detachment through the constrained contractile force between adjacent cells in the contiguous cell monolayers. On the other hand, polyelectrolyte-modified indium tin oxide (ITO) electrodes allowed for cell growth and cell sheet detachment upon electrochemical trigger (Guillaume-Gentil et al. 2008). This latter approach relied on the electrochemically-induced dissolution of polyelectrolyte multilayers or electrochemical desorption of polyelectrolyte monolayers, with the polyelectrolyte coatings serving as sacrificial cell substrates.

Native tissues comprise multiple cell types assembled in a complex, well-defined architecture in which cell-cell interactions have a profound influence on the function and fate of each individual cell, and hence on the overall tissue properties. The engineering of platforms allowing for the co-culture of multiple cell types mimicking the *in vivo* spatial arrangement of cells *in vitro* is therefore a prerequisite for the reconstruction of functional tissue-like structures. In addition, recreating the heterotypic configuration of native tissue also has a high relevance for the creation of *in vitro* cell culture systems which better maintain the physiologic functions of cells found *in vivo*.

Allowing for the creation of 3D cellular constructs by stacking harvested cell sheets, cell sheet-based tissue engineering constitutes a promising approach for the engineering of complex 3D cellular assemblies resembling native tissues (Elloumi-Hannachi et al. 2010).

While overlaying cell sheets of different cell types readily allows for the formation of heterotypic constructs, even more precise spatial organization can be attained by micro-structuring multiple cell types within the individual cell sheets.

In the present work, tunable cell adhesivity and electrochemical dissolution of polyelectrolyte substrates, previously developed for cell sheet engineering (Guillaume-Gentil et al. 2008), are combined into a novel approach for the micro-patterning and harvesting of heterotypic cell sheets.

Several strategies have been previously developed for the creation of micro-patterned cell co-cultures systems. Early approaches relied on the preferential attachment of one particular cell type (i.e. hepatocytes or astrocytes) on defined proteins or polyelectrolyte micro-patterns obtained by photolithography (Bhatia et al. 1997, 1998, 1999), micro-fluidic (Folch and Toner 1998), or micro-contact printing (Kidambi et al. 2007, 2008), and the subsequent seeding of a more adhesive second cell type. A second generation of micro-patterning systems made use of physical barriers that could be removed after the attachment of a first cell population, rendering the techniques suitable for any combination of cell types. The reversible sealing of microfluidic systems (Folch et al. 1999; Chiu et al. 2000) or elastomeric stencils (Folch et al. 2000; Ostuni et al. 2000; Wright et al. 2007) were thus used to prevent locally the attachment of the first cell type. Alternatively, a recently-developed micromechanical strategy enabled the spatial organization of different cell populations by growing a different cell type on two individual interlocking plates which could be precisely positioned together or with a gap, allowing for dynamic co-cultures with tunable micro-spacing between the different cell types (Hui and Bhatia 2007). Lastly, strategies based on dynamic platforms were developed, where non adhesive micro-domains can be switched to cell adhesive after the adhesion of the first cell population, allowing to control both spatially and temporally the biointerfacial properties of the substrate. Non-fouling micro-patterns of hyaluronic acid created by capillary force lithography were subsequently complexed with poly-L-lysine or collagen, switching the domains properties to cell adhesive (Khademhosseini et al. 2004; Fukuda et al. 2006). Electron beam irradiation through a metal mask allowed for the fabrication of micro-domains grafted with thermally reversible polymers which can be switched from hydrophilic, cell repellent to hydrophobic, cell adhesive upon variation in temperature (Yamato et al. 2001, 2002; Tsuda et al. 2005, 2006). Electroactive self-assembled monolayers micro-patterned on gold electrodes by micro-contact printing could be switched from cell-repellent to cell adhesive upon electrochemical oxidation (Yousaf et al. 2001; Lee et al. 2009). Finally, a recent work reported the creation of micro-patterned co-cultures using non-fouling micro-domains of self-assembled poly(ethylene glycol) silane monolayers which could be electrochemically desorbed from an ITO electrode substrate after attachment of the first cell population (Shah et al. 2009).

The alternative approach presented in this article is based on the selective dissolution of polyelectrolyte mono- or multilayers from indium tin oxide electrodes with micro-patterned insulating domains. This new platform enables a precise spatio-temporal control over the biointerface properties, while providing high versatility and simplicity. Furthermore, the possibility for a final harvesting of the micro-structured heterotypic cell sheets offers great prospects for future application in cell sheet-based tissue engineering. This novel approach is thus appealing not only for the creation of 2D functional co-cultures systems, but also for the creation of 3D tissue-like constructs replicating the complex hierarchical organization of native tissues.

2 Materials and methods

2.1 Polyelectrolytes and solutions

Poly-L-lysine hydrobromide (PLL, Mw ~15–30 kDa) and hyaluronic acid sodium salt from bovine vitreous humor (HA, Mw ~300 kDa) were purchased from Sigma Aldrich (Buchs, Switzerland). Poly(L-lysine)-graft-(polyethylene glycol) with a PLL backbone chain of 20 kDa, 2 kDa PEG side chains and a grafting ratio of 3.5, and RGD-grafted poly(L-lysine)-graft-(polyethylene glycol) copolymer with a PLL backbone chain of 20 kDa, 2 kDa unfunctionalized PEG side chains, 3.4 kDa longer PEG side chains carrying the RGD ligand and a grafting ratio of 3.4, were obtained from SurfaceSolutionS GmbH (Zurich, Switzerland); the polymers are later abbreviated as PLL-*g*-PEG and PLL-*g*-PEG/PEG-RGD respectively. All the polymers were used at a concentration of 0.5 mg/ml in HEPES-2 buffer solution. Fibronectin from human plasma (FN) was purchased from Roche Diagnostics GmbH (Mannheim, Germany) and used at a concentration of 0.05 mg/ml in HEPES-2 buffer solution. All solutions were filtered through 0.22 μm pore size filters before use. HEPES-2 buffer was prepared with 10 mM 4-(2-hydroxyethyl)piperazine-1-ethanesulfonic acid (HEPES, Fluka, Buchs, Switzerland) supplemented with 150 mM sodium chloride (Fluka, Buchs, Switzerland) in ultra-pure water filtered through MilliQ Gradient A10 filters (Millipore AG, Switzerland), with a pH adjusted to 7.4 using 6 M NaOH (Fluka, Buchs, Switzerland).

2.2 Cell culture and live-cell labeling

C_2C_{12} mouse myoblasts and human mesenchymal stem cells were purchased from American Type Culture Collection (LGC Standards, Molsheim, France) and Lonza (Verviers, Belgium) respectively. Bovine chondrocytes were isolated from knees of 6 month old calves using a pronase/collagenase digestion. Healthy human cartilage was obtained from surgical procedures at the University Hospital Zürich according to ethical guidelines and chondrocytes were isolated using a pronase/collagenase digestion. All cells were maintained at 37°C, 7% CO_2 atmosphere in growth medium consisting of Dulbecco's modified eagle's media (DMEM, Invitrogen, Switzerland) supplemented with 10% fetal bovine serum (FBS, Invitrogen, Switzerland) and 1% penicillin/streptomycin (Invitrogen, Switzerland). For fluorescent labeling of living cells, adherent cells were trypsinized, washed one time with pure DMEM, and incubated for 30 min at 37°C, 7% CO_2 in DMEM supplemented with 1–2 μM 5-(and-6)-(((4-chloromethyl) benzoyl)amino)tetramethylrhodamine (CellTracker™ Orange CMTMR, Molecular Probes, Invitrogen, Switzerland) or 1–2 μM 5-chloromethylfluorescein diacetate (CellTracker™ Green CMFDA, Molecular Probes, Invitrogen, Switzerland). The labeled cells were resuspended in growth medium and counted with a Countess® Automated Cell Counter (Invitrogen, Switzerland) before seeding at 150,000–400,000 cells/cm^2 on the micro-structured substrates.

2.3 Photoresist patterning on ITO electrodes

Glass wafers (63.5 mm×63.5 mm×0.5 mm) coated with a ~50 nm thick indium tin oxide (ITO) layer (Microvacuum, Hungary) were cleaned by 10 min ultrasonication in isopropanol, 10 min ultrasonication in Millipore water, N_2-blow drying, and 2 min O_2 plasma treatment. The ITO coated substrates were then placed on a heating plate at 150°C for 20 min to remove adsorbed water and improve the photoresist adhesion. After cooling down to room temperature, a negative photoresist (SU-8, GM1040, Gersteltec, Switzerland) was spin coated on the wafers at 500 rpm for 40 s, and the substrates were soft baked (10 min, 65°C; ramped to 95°C at 2°C/min; 30 min, 95°C). A Karl Süss X380 mask aligner was used as a UV source and the photoresist was illuminated for 26 s through a mask, and post-baked with the same temperature profile as used for the soft baking. The SU-8 structure was developed in 2-methoxy-1-methylethyl acetate (PGMA) for 2 min, rinsed with isopropanol and dried at ambient air, before hard baking at 135°C for 2 h on a hot plate. The wafers with SU-8 micro-structures were finally diced into 24 mm×24 mm chips.

2.4 Electrochemistry

All electrochemical experiments were performed using a teflon electrochemical liquid-cell provided with a three electrode configuration system: the ITO surface of the substrate contacted with a metallic copper spring served as working electrode, a silver wire was used as Ag/AgCl reference electrode, and a platinum wire as counter electrode. As electrolyte solutions, HEPES-2 buffer was used for electrochemical treatments without cells, while cell growth medium supplemented with 3 mM HEPES was used for the samples with cells. The electrochemical stimuli were applied using an AMEL potentiostat/galvanostat (model 2053, AMEL electrochemistry, Italy).

2.5 Surface modification with polyelectrolytes

Shortly prior polyelectrolyte adsorption, the chips were cleaned by ultrasonication for 10 min in isopropanol and 10 min in ultrapure water, drying with filtered nitrogen, followed by 2 min oxygen plasma treatment, and cyclic voltammetry in HEPES-2 buffer (5 cycles between 0 and

2 V). PLL and HA layers were adsorbed by substrate immersion for 20 min in the respective polyelectrolyte solution followed by three rinsing steps in HEPES-2 buffer, starting with a polycation layer and alternating polycation and polyanion deposition until formation of the desired coating. Additional layer of fibronectin or PLL-*g*-PEG/PEG-RGD, onto PLL or HA-outermost layers respectively, was assembled through a 45 min dipping step followed by three rinsing steps in HEPES-2. For the investigation of the selective polyelectrolyte dissolution by electrochemical atomic force microscopy, the $(PLL/HA)_6$ multilayers were alternatively deposited by spraying technology, using a custom made automated spraying system described elsewhere (Guillaume-Gentil et al. 2010). All polyelectrolytes were sprayed on the samples tilted at 45°, from a distance of 19±2 cm and at a constant pressure of 1 bar for 5 s, followed by a pause of 15 s, spraying of HEPES-2 buffer for 5 s, and a pause of 5 s.

2.6 Monitoring of local polyelectrolyte electrochemical dissolution by electrochemical atomic force microscopy (ecAFM)

A Nanowizard I BioAFM (JPK Instruments, Germany) and Mikromasch CSC38/noAl cantilevers were used. The samples mounted in the electrochemical liquid-cell were scanned both in contact and intermittent-contact fluid modes. At first, polyelectrolyte-coated samples were scanned at different locations on ITO, SU-8, and mixed domains. The samples were then subjected to an electrochemical stimulus (15 μA/cm² for 15 min), followed by new imaging of the local areas previously scanned. Electrochemical and imaging steps were repeated until nearly complete dissolution of the polyelectrolytes from the ITO domains. No rinsing of the samples was performed. The obtained ecAFM height mode images were further processed using SPM image processing software (JPK Instruments, Germany). Processed images were exported as ASCII files for calculation of the adsorbed volume in MatLab. As AFM output data is pixilated the simplest way to calculate the volume was to multiply each pixel value with its area to create one pixel volume. The pixel volumes were then added together to represent the entire volume of the PEM structures.

2.7 Micro-patterning polyelectrolytes and homotypic cell cultures

Micro-patterned electrode substrates were coated with the desired polyelectrolytes and subjected to a current density of 15 μA/cm² for 30 to 60 min, under constant rinsing with HEPES-2 buffer, in order to remove polyelectrolytes from the non-insulated ITO domains. As a backfilling step to render the ITO domains cell-resistant, the samples were then incubated for 45 min with a PLL-*g*-PEG solution and rinsed three times with HEPES-2 buffer. Prior to cell seeding, the substrates were shortly rinsed with a 70% ethanol solution, and rinsed three times with sterile filtered HEPES-2 buffer and three times with cell growth medium. Cells were then seeded at densities ranging from 150,000 to 400,000 cells/cm², and the samples were incubated for 20–30 min under normal cell culture conditions before rinsing with growth medium to wash away non-adherent cells.

2.8 Electrochemical desorption of PLL-g-PEG and formation of heterotypic co-cultures

For the creation of heterotypic co-cultures, the samples with micro-patterned homotypic cultures were first subjected to electrochemical treatment to remove the non-fouling PLL-*g*-PEG layer. A current density of 15 μA/cm² was then applied for 15 min, in cell growth medium supplemented with 3 mM HEPES. The electrochemical desorption of PLL-*g*-PEG was immediately followed by sample incubation for 15 min with a PLL-*g*-PEG/PEG-RGD solution at 37°C, 7% CO_2. The samples were then rinsed three times with HEPES-2 and three times with cell growth medium, and let incubated under normal cell culture conditions until next cell seeding. The second cell population was seeded at densities ranging from 150,000 to 400,000 cells/cm², and the non-adherent cells were washed away upon rinsing with growth medium after 20–30 min incubation under normal cell culture conditions.

2.9 Electrochemically-induced detachment of heterotypic cell sheets

Samples with a micro-patterned co-culture were incubated for 1 day under normal cell culture conditions, allowing for cell growth and the establishment of cell-cell contacts. An electrochemical treatment (15 min at 15 μA/cm² in growth medium supplemented with 3 mM HEPES) was then applied, inducing the detachment of the heterotypic cell sheets, starting from the periphery. Rinsing of the samples with growth medium aided the detachment of the cell monolayer.

2.10 Fluorescence and phase contrast microscopy

Phase contrast and fluorescence microscopy images were acquired using an inverted microscope (DM IL, Leica Microsystems Ltd, Switzerland).

3 Results and discussion

In this study, a novel approach for the micro-patterning and consecutive detachment of heterotypic cell sheets is

presented, based on the spatially controlled electrochemical dissolution of polyelectrolyte coatings (see Fig. 1).

The micro-patterned substrates with SU-8 insulating domains and the selective electrochemical dissolution of polyelectrolytes from non-insulated domains were characterized by ecAFM. The micro-patterning of polyelectrolytes and homotypic myoblast or chondrocyte cultures, and the creation and harvesting of chondrocyte-mesenchymal stem cell co-cultures demonstrated the versatility and potency of this technique for future applications in tissue engineering.

3.1 Creation of insulated domains and selective polyelectrolyte dissolution

At first, insulated micro-patterns were created on indium tin oxide electrodes by photolithography, using a negative photoresist (SU-8) (Fig. 1(a–b)). The obtained SU-8 adlayer presented well resolved micro-structures and had a thickness of about 2.3 μm as determined by AFM measurements (Fig. 2(a)). To demonstrate the insulating properties of the micro-structured SU-8 adlayer, hence the possibility for a selective polyelectrolyte dissolution from the non-insulated ITO micro-domains (Fig. 1(c–d)), a micro-patterned substrate coated with a $(PLL/HA)_6$ multilayer was subjected to a current density of 15 μA/cm² for 30 min and the electrochemically induced dissolution of the polyelectrolyte coating was followed locally, *in situ*, by ecAFM (Fig. 2(b–c)). On both ITO and SU-8 domains, the deposited polyelectrolytes formed nano-droplets complexes, with heights ranging from 40 to 100 nm. Upon the electrochemical trigger, the PLL/HA nano-droplets on the ITO domains dissolved, with less than 15% residual volume after 30 min (Fig. 2(b)). The polyelectrolyte nano-structures on the SU-8 micro-patterns remained however unaffected, with no changes in the coating morphology or in the volume of polyelectrolyte adsorbed (Fig. 2(c)). These results demonstrate that the electrochemical detachment of the polyelectrolytes is highly localized to the conductive areas. Previous studies (Guillaume-Gentil et al. 2010; Boulmedais et al.

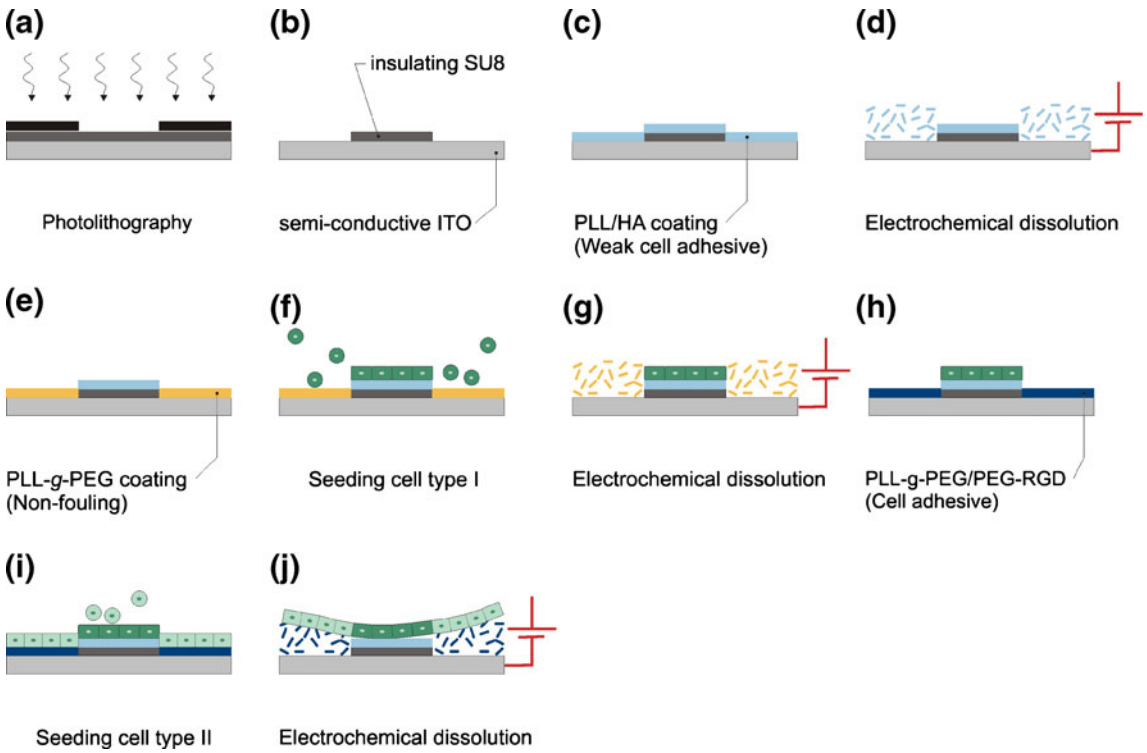

Fig. 1 Micro-patterning heterotypic cell sheets based on local electrochemical dissolution of polyelectrolyte coatings. (**a**) A SU-8 layer spin-coated on an indium tin oxide (ITO) electrode is exposed to UV light through a mask. (**b**) After development, SU-8 micro-patterns with insulating properties are formed on the ITO electrode. (**c**) The whole substrate is coated with a weak cell adhesive polyelectrolyte multilayer. (**d**) The sample is subjected to electrochemical polarization, inducing polyelectrolyte dissolution only from the ITO domains. (**e**) The bare ITO domains are backfilled with PLL-*g*-PEG, a cell-resistant polymer. (**f**) A first cell population is seeded, and non-adherent cells are washed away. (**g**) A second electrochemical step allows for the removal of the non-fouling PLL-*g*-PEG monolayer from the ITO domains. (**h**) The bare ITO domains are backfilled with a cell adhesive PLL-*g*-PEG/PEG-RGD monolayer. (**i**) The second cell population is seeded, and non-adherent cells are washed away. (**j**) After one day growth, a final electrochemical step allows for cell sheet detachment through the dissolution of the PLL-*g*-PEG/PEG-RGD monolayer. The cells on the weak cell adhesive domains also detach easily because the cohesion between the cells is bigger than their interaction with the substrate

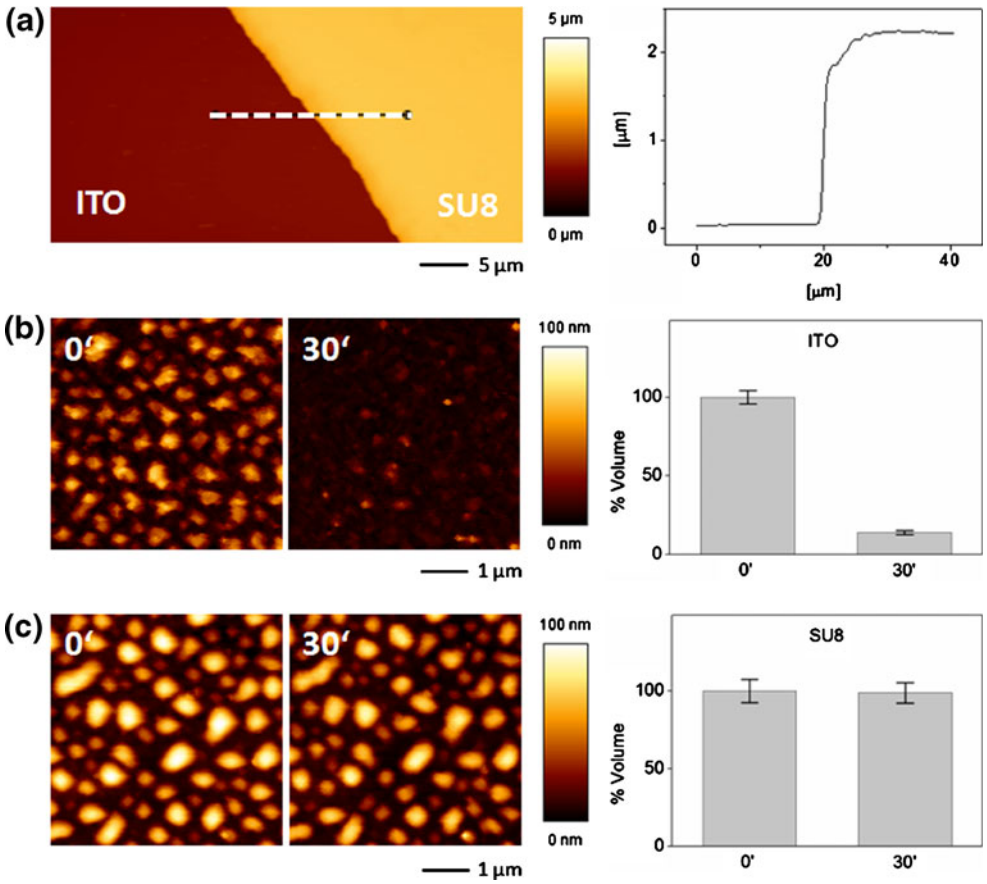

Fig. 2 Selective polyelectrolyte dissolution upon electrochemical treatment. (**a**) AFM height mode image (80×40 µm²) of a micro-structured SU-8 adlayer on an ITO electrode. The profile (right) corresponds to the white dash line drawn on the AFM image. (**b**) AFM height mode images (10×10 µm²) of a $(PLL/HA)_6$-coated ITO domain initially (0') and after electrochemical treatment (30'). The graph on the right side represents the percentage of initial volume of polyelectrolyte adsorbed calculated from four AFM images, with standard errors of mean as error bars. (**c**) AFM height mode images (10×10 µm²) of a $(PLL/HA)_6$-coated SU-8 domain initially (0') and after electrochemical treatment (30'). The graph on the right side represents the percentage of initial volume of adsorbed polyelectrolyte calculated from four AFM images, with standard errors of mean as error bars

2006; Gabi et al. 2009) reported that the applied electrochemical treatment induces the electrolysis of water, hence the continuous production of protons at the electrode surface. The resulting pH lowering, which instigates the dissolution of the polyelectrolyte multilayer, has been shown to remain locally confined, extending only to a few hundreds of nanometers above the ITO electrode in our experimental conditions. Thus, while sufficient to trigger the disassembly of nanometer-scale polyelectrolyte structures adsorbed directly on the ITO electrode, the electrochemical treatment did not affect the bulk solution or the polyelectrolytes on the neighboring SU-8 domains.

3.2 Micro-patterning of polyelectrolytes and cells

Based on the selective dissolution of polyelectrolyte coatings (from ITO but not from SU-8 insulated domains), cytophilic/cytophobic micro-patterned substrates were created (Fig. 1(c–e)). At first, ITO substrates with SU-8 micro-structures were coated with polyelectrolyte coatings, with an outermost layer preventing the adsorption of PLL-*g*-PEG, e.g. a positive PLL terminal layer or final adsorption of fibronectin or PLL-*g*-PEG/PEG-RGD. The substrates were then subjected to a current density of 15 µA/cm² for 30–60 min in order to remove the polyelectrolytes from the non-insulated ITO domains. In a final backfill dip-and-rinse step, non-functionalized PLL-*g*-PEG was adsorbed on the ITO background, rendering it resistant to cell attachment (Elbert and Hubbell 1998). The substrates were then incubated with mammalian cells for 20–30 min. The cells attached on the micro-patterned polyelectrolyte-coated SU-8 domains, and the non-adherent cells which sedimented on the PLL-*g*-PEG domains were washed away upon rinsing (Fig. 3(a–b)). In Fig. 3 (b–j) a sampling of homotypic micro-patterned culture of myoblasts or chondrocytes obtained with this technology is shown, with patterns of different geometries and sizes ranging from 50 µm to 2 mm. The patterns of adherent cells reproduced the design of the polyelectrolyte-coated SU-8 stencil with high fidelity, with a minimal cell attachment on the pegylated ITO domains. SU-8 has been previously reported to be compatible with cell cultures (Voskerician et al. 2003). Here, the different cell types showed a good adhesion onto the polyelectrolyte-coated SU-8 structures, and no adverse effect was observed on the cells cultured on the micro-patterned substrates.

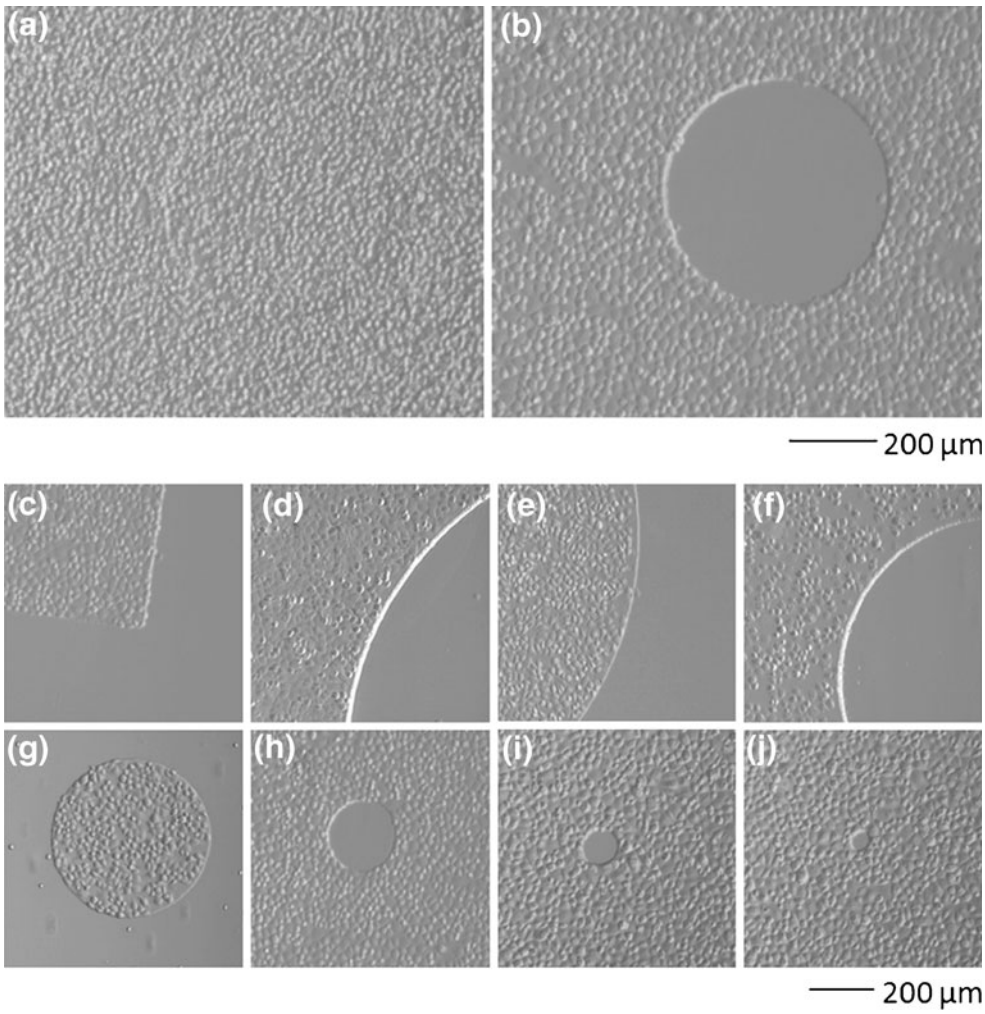

Fig. 3 Cell micro-patterning on SU-8 domains with various cell adhesive coatings and a non-fouling PLL-*g*-PEG coated ITO background. (**a**) C_2C_{12} myoblasts 20 min after seeding at 400,000 cells/cm^2 on SU-8 coated with PLL-FN with a 500 µm patterned hole. After rinsing (**b**), the cells attached on PLL-FN remained, while cells on the PLL-*g*-PEG domain were washed away. (**c**, **h**) C_2C_{12} on PLL-FN, 20 min after seeding at 400,000 cells/cm^2. (**d**) Human chondrocytes on $(PLL\text{-}HA)_3$-PLL-*g*-PEG/PEG-RGD 2 h30 after seeding at 300,000 cells/cm^2. (**e**, **g**) C_2C_{12} on PLL 60 min after seeding at 300,000 cells/cm^2. (**f**) Human chondrocytes on (PLL-HA)-PLL-*g*-PEG/PEG-RGD 30 min after seeding at 300,000 cells/cm^2. (**i-j**) Human chondrocytes on PLL-FN 1 h15 after seeding at 150,000 cells/cm^2

3.3 Electrochemical switching of ITO domains and formation of micro-patterned co-cultures

The addition of a second cell type to the same micro-structured substrate required a switch of the surface properties of the ITO domains from non-fouling to cell adhesive. The samples with the first cell population on the SU-8 micro-patterns defined on a cell-resistant PLL-*g*-PEG background were thus further subjected to electrochemical polarization. A current density of 15 µA/cm² was applied for 15 min, leading to desorption of the PLL-*g*-PEG monolayer from the conducting areas. The cells attached on the SU-8-insulated domains were not affected by the electrochemical treatment. As previously discussed, the electrochemical reactions triggering polyelectrolyte dissolution occur locally at the ITO interface, without affecting the bulk solution or the insulated areas. The bare ITO domains unveiled through the electrochemical treatment could then be coated with a cell adhesive PLL-*g*-PEG/PEG-RGD monolayer simply by incubation with an aqueous solution of the polymer. The incubation of the samples with human mesenchymal stem cells or myoblasts resulted in a rapid, selective attachment of the cells to the RGD-functionalized domains, while cell adhesion onto the first cell population remained poor. Non-adherent cells were washed away upon rinsing of the samples. Figure 4 shows micro-patterned co-cultures of primary human chondrocytes and human mesenchymal stem cells achieved using this approach. While an RGD-functionalized PLL-*g*-PEG copolymer was used as cell adhesive, electrochemically

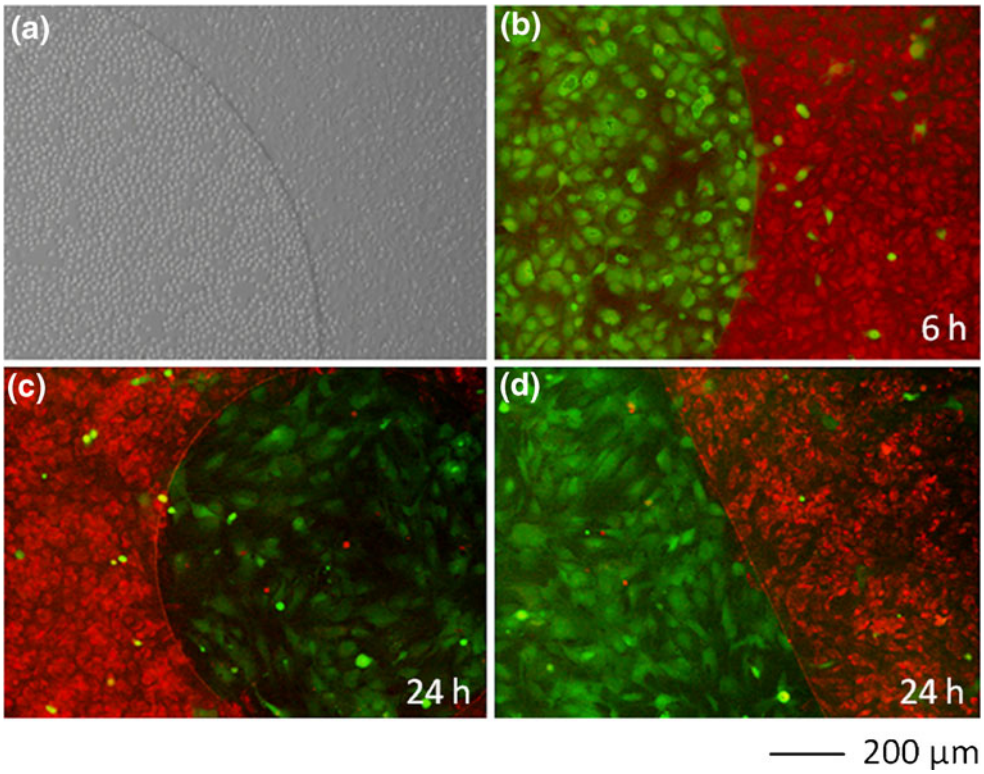

Fig. 4 Micro-patterned co-cultures of primary human chondrocytes and human mesenchymal stem cells. (**a**) Micro-pattern of human chondrocytes grown for 3.5 h on PLL-HA-PLL-*g*-PEG/PEG-RGD (right) and freshly seeded hMSCs on PLL-*g*-PEG/PEG-RGD (left). (**b**) hMSCs (green) grown for 3 h on PLL-*g*-PEG/PEG-RGD next to human chondrocytes (red) cultured for 6 h on PLL-HA-PLL-*g*-PEG/PEG-RGD. Circular (**c**) and line patterns (**d**) of human MSCs on PLL-*g*-PEG/PEG-RGD (green) co-cultured with human chondrocytes on PLL-HA-PLL-*g*-PEG/PEG-RGD (red) after 24 h growth

desorbable substrate for the second cell type, versatility can be added to this platform by modifying the PEG chains of the PLL-*g*-PEG polymer with a variety of other bioactive molecules. Furthermore, the surface density can be tailored during polymer synthesis by adjusting the grafting ratio or by mixing functionalized and non-functionalized polymers with at different molar ratio (Faraasen et al. 2003; Huang et al. 2001; Tosatti et al. 2003; Zhen et al. 2006).

3.4 Detaching heterotypic cell sheets

The micro-patterned cell co-cultures obtained with this electrochemical approach had ultimately two different types of underlying substrates. The first cell type was grown on (PLL/HA)-based polyelectrolyte domains, insulated from the electrode by a thin SU-8 layer. Such polyelectrolyte coatings have been shown to present relatively weak cell

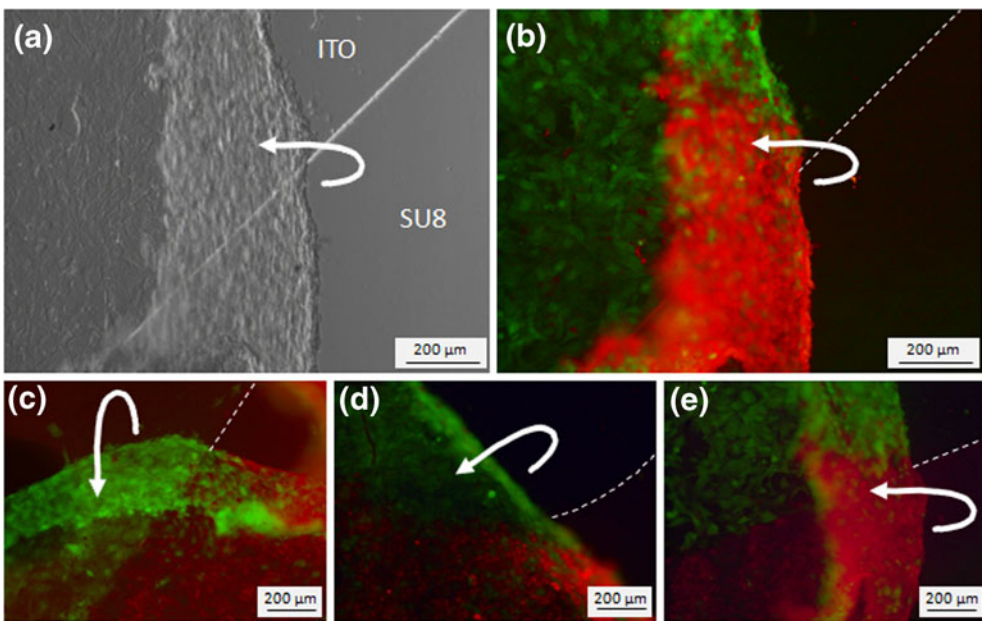

Fig. 5 Electrochemically-induced detachment of human chondrocyte (red) and human mesenchymal stem cell (green) co-cultures, grown for one day on PLL-HA-PLL-*g*-PEG/PEG-RGD and PLL-*g*-PEG/PEG-RGD, respectively. The white dashed line on each fluorescence microscopy image shows the border of the SU-8 microstructure, and the white arrow indicates the peeling of the heterotypic cell sheet. (**a** and **b**) are contrast and fluorescence microscopy images of the same region of one sample. (**c**-**e**) are images of detaching and folding cell-sheets of various other samples

adhesive properties (Weder et al. 2010) and to allow for cell sheet detachment through the contractile forces exerted between adjacent cells in a dense cell monolayer once cell-cell contacts have been established (Guillaume-Gentil et al. 2008). The second type attached on highly cell adhesive domains through a PLL-*g*-PEG/PEG-RGD monolayer adsorbed electrostatically on the ITO electrode. It has been shown previously (Guillaume-Gentil et al. 2008) that cells can be released as intact sheets from such substrate upon electrochemical dissolution of the sacrificial PLL-*g*-PEG/PEG-RGD monolayer. Therefore, in order to harvest micro-patterned cell sheets, the co-cultures were grown for one day and subjected to electrochemical treatment (15 min at 15 μA/cm²). Inducing the PLL-*g*-PEG/PEG-RGD desorption, the electrochemical trigger instigated the detachment of the entire heterotypic cell sheets, with the cells on insulated domains following the detachment as a result of their weak interaction with the substrate and the strong interactions with neighboring cells. Figure 5 shows examples of co-cultures of primary human chondrocytes and human mesenchymal stem cells detaching from the micro-structured substrate upon electrochemical stimulation, with preservation of the heterotypic cell-cell contacts. In these experiments the obtained cell sheet folds onto itself because of the internal stress of the cells. However, this could be easily avoided using gel stamps that support the cell-sheet during detachment as previously shown by the Okano group (Sasagawa et al. 2010).

4 Conclusions and outlook

The strategy described in this article allowed for the micro-patterning of both homotypic cell cultures and heterotypic cell co-cultures, as well as for controlled detachment of the micro-structured cell co-cultures. Combining the precision of SU-8 photolithographic processing and the localized nature of the electrochemically-induced dissolution of polyelectrolytes, this approach allowed for an accurate spatial and temporal control over the cell attachment on the micro-structured substrates. The potential of this cell micro-patterning strategy was demonstrated with several cell types, including human mesenchymal stem cells, primary chondrocytes and a myoblastic cell line. This simple, versatile platform offers great prospects for future tissue engineering applications, with the overlaying of harvested micro-patterned co-cultures allowing for the design of 3D cellular constructs mimicking the complex architecture of tissues *in vivo*.

Future work will include the application of this micro-patterning approach to electrode arrays through preliminary etching of the ITO layer, to assess the possibility of multiple, separately addressable electrodes for the micro-patterning of more than two cell types.

Acknowledgements The authors thank Stephen Wheeler and Martin Lanz for technical assistance and the Competence Centre for Material Science and Technology (CCMX), ETH Zurich, the Marie Heim-Vögtlin grant No. PMPDP2_122997 from the Swiss National Science Foundation, and the European Union Seventh Framework Programme (FP7/2007-2013) under grant agreement n° NMP4-SL-2009-229292 (Find&Bind) for financial support.

References

S.N. Bhatia, M.L. Yarmush, M. Toner, J. Biomed. Mater. Res. **34**, 189–199 (1997)
S.N. Bhatia, U.J. Balis, M.L. Yarmush, M. Toner, Biotechnol. Prog. **14**, 378–387 (1998)
S.N. Bhatia, U.J. Balis, M.L. Yarmush, M. Toner, FASEB J. **13**, 1883–1900 (1999)
T. Boudou, T. Crouzier, K. Ren, G. Blin, C. Picart, Adv. Mater. **22**, 441–467 (2010)
F. Boulmedais, C.S. Tang, B. Keller, J. Vörös, Adv. Funct. Mater. **16**, 63–70 (2006)
D.T. Chiu, N.L. Jeon, S. Huang, R.S. Kane, C.J. Wargo, I.S. Choi, D. E. Ingber, G.M. Whitesides, Proc. Natl Acad. Sci. USA **97**, 2408–2413 (2000)
G. Decher, Science **277**, 1232–1237 (1997)
D.L. Elbert, J.A. Hubbell, Chem. Biol. **5**, 177–183 (1998)
I. Elloumi-Hannachi, M. Yamato, T. Okano, J. Intern. Med. **267**, 54–70 (2010)
S. Faraasen, J. Vörös, G. Csúcs, M. Textor, H.P. Merkle, E. Walter, Pharm. Res. **20**, 237–246 (2003)
A. Folch, M. Toner, Biotechnol. Prog. **14**, 388–392 (1998)
A. Folch, A. Ayon, O. Hurtado, M.A. Schmidt, M. Toner, J. Biomech. Eng. **121**, 28–34 (1999)
A. Folch, B.-H. Jo, O. Hurtado, D.J. Beebe, M. Toner, J. Biomed. Mater. Res. **52**, 346–353 (2000)
J. Fukuda, A. Khademhosseini, J. Yeh, G. Eng, J. Cheng, O.C. Farokhzad, R. Langer, Biomaterials **27**, 1479–1486 (2006)
M. Gabi, T. Sannomiya, A. Larmagnac, M. Puttaswamy, J. Vörös, Integr. Biol. **1**, 108–115 (2009)
O. Guillaume-Gentil, Y. Akiyama, M. Schuler, C. Tang, M. Textor, M. Yamato, T. Okano, J. Vörös, Adv. Mater. **20**, 560–565 (2008)
O. Guillaume-Gentil, N. Graf, F. Boulmedais, P. Schaaf, J. Vörös, T. Zambelli, Soft Matter **6**, 4246–4254 (2010)
N.-P. Huang, J. Vörös, S.M. De Paul, M. Textor, N.D. Spencer, Langmuir **18**, 220–230 (2001)
E.E. Hui, S.N. Bhatia, Proc. Natl. Acad. Sci. **104**, 5722–5726 (2007)
A. Khademhosseini, K.Y. Suh, J.M. Yang, G. Eng, J. Yeh, S. Levenberg, R. Langer, Biomaterials **25**, 3583–3592 (2004)
S. Kidambi, L. Sheng, M.L. Yarmush, M. Toner, I. Lee, C. Chan, Macromol. Biosci. **7**, 344–353 (2007)
S. Kidambi, I. Lee, C. Chan, Adv. Funct. Mater. **18**, 294–301 (2008)
E.-J. Lee, E.W.L. Chan, M.N. Yousaf, Chembiochem **10**, 1648–1653 (2009)
E. Ostuni, R. Kane, C.S. Chen, D.E. Ingber, G.M. Whitesides, Langmuir **16**, 7811–7819 (2000)
C. Picart, P. Lavalle, P. Hubert, F.J.G. Cuisinier, G. Decher, P. Schaaf, J.C. Voegel, Langmuir **17**, 7414–7424 (2001)
C. Picart, J. Mutterer, L. Richert, Y. Luo, G.D. Prestwich, P. Schaaf, J. C. Voegel, P. Lavalle, Proc. Natl Acad. Sci. USA **99**, 12531–12535 (2002)
T. Sasagawa, T. Shimizu, S. Sekiya, Y. Haraguchi, M. Yamato, Y. Sawa, T. Okano, Biomaterials **31**, 1646–1654 (2010)

J.B. Schlenoff, S.T. Dubas, T. Farhat, Langmuir **16**, 9968–9969 (2000)
S.S. Shah, M.C. Howland, L.-J. Chen, J. Silangcruz, S.V. Verkhoturov, E.A. Schweikert, A.N. Parikh, A. Revzin, ACS Appl. Mater. Interfaces **1**, 2592–2601 (2009)
Z. Tang, Y. Wang, P. Podsiadlo, N.A. Kotov, Adv. Mater. **18**, 3203–3224 (2006)
S. Tosatti, S.M.D. Paul, A. Askendal, S. VandeVondele, J.A. Hubbell, P. Tengvall, M. Textor, Biomaterials **24**, 4949–4958 (2003)
Y. Tsuda, A. Kikuchi, M. Yamato, A. Nakao, Y. Sakurai, M. Umezu, T. Okano, Biomaterials **26**, 1885–1893 (2005)
Y. Tsuda, A. Kikuchi, M. Yamato, G. Chen, T. Okano, Biochem. Biophys. Res. Commun. **348**, 937–944 (2006)
S. VandeVondele, J. Vörös, J.A. Hubbell, Biotechnol. Bioeng. **82**, 784–790 (2003)
G. Voskerician, M.S. Shive, R.S. Shawgo, H.V. Recum, J.M. Anderson, M.J. Cima, R. Langer, Biomaterials **24**, 1959–1967 (2003)
G. Weder, O. Guillaume-Gentil, N. Matthey, F. Montagne, H. Heinzelmann, J. Vörös, M. Liley, Biomaterials **31**, 6436–6443 (2010)
D. Wright, B. Rajalingam, S. Selvarasah, M.R. Dokmeci, A. Khademhosseini, Lab Chip **7**, 1272–1279 (2007)
M. Yamato, O.H. Kwon, M. Hirose, A. Kikuchi, T. Okano, J. Biomed. Mater. Res. **55**, 137–140 (2001)
M. Yamato, C. Konno, M. Utsumi, A. Kikuchi, T. Okano, Biomaterials **23**, 561–567 (2002)
M.N. Yousaf, B.T. Houseman, M. Mrksich, Proc. Natl Acad. Sci. USA **98**, 5992–5996 (2001)
G. Zhen, D. Falconnet, E. Kuennemann, J. Vörös, N. Spencer, M. Textor, S. Zürcher, Adv. Funct. Mater. **16**, 243–251 (2006)